Analysis of Tilt-to-length Coupling Noise: Exploring the Influence of Multiple Factors in the Test Mass Interferometer

Mengyuan Zhao[1,2#], Jia Shen[3,4#], Xiaodong Peng[2,5,6,7], Xiaoshan Ma[8*], Zhen Yang[2], Heshan Liu[3], Xin Meng[2] and Jiafeng Zhang[2,4]

[1]*School of Information, Xi'an University of Finance and Economics, Xi'an 710100, P.R. China*

[2]*Key Laboratory of Electronics and Information Technology for Space System, National Space Science Center, Chinese Academy of Sciences, Beijing 100190, P.R. China*

[3]*Institute of Mechanics, Chinese Academy of Sciences, Beijing 100190, P.R. China*

[4]*University of Chinese Academy of Sciences, Beijing 100049, P.R. China*

[5]*Taiji Laboratory for Gravitational Wave Universe, Hangzhou 310024, P.R. China*

[6]*Key Laboratory of Gravitational Wave Precision Measurement of Zhejiang Province, Hangzhou 310024, P.R. China*

[7]*School of Fundamental Physics and Mathematical Sciences, Hangzhou Institute for Advanced Study, UCAS, Hangzhou 310024, P.R. China*

[8]*Institute of Engineering Thermophysics, Chinese Academy of Sciences, Beijing 100190, P.R. China*

[#]*Co-first author*
[*]*Corresponding author, E-mail: maxiaoshan@iet.cn*

Abstract: For space-borne gravitational wave detection missions based on heterodyne interferometry principle, tilt-to-length (TTL) coupling noise is an important optical noise source, exerting significant influence on the accuracy of the measurement system. This paper presents a method for analyzing TTL coupling noise under the joint influence of multiple factors. An equivalent simulated optical bench for the test mass interferometer is designed here, and the Gaussian beam tracing is adopted to simulate beam propagation. By simulating the interference signal, it is capable of analyzing the impact of various factors on the TTL coupling noise, including positional, beam parameters, detector parameters, and signal definition factors. On this basis, a random parameter space composed of multiple influential factors is constructed within a range satisfying the analysis requirement, and the corresponding simulation results from randomly sampling are evaluated via

variance-based global sensitivity analysis. The calculated results of the main effect index and the total effect index show that the test mass rotation angle and the piston effect -lateral have significant influence on the TTL coupling noise in the test mass interferometer. The analysis provides qualitative reference for the design and optimization of space-borne laser interferometry system.

Key words: space interferometry; optical simulation; tilt-to-length coupling

测试质量干涉仪抖动光程耦合噪声的多因素影响分析

赵梦园[1,2#]，沈嘉[3,4#]，彭晓东[2,5,6,7]，马晓珊[8*]，杨震[2]，刘河山[3]，孟新[2]，张佳锋[2,4]

1（西安财经大学 信息学院，陕西 西安 710100）
2（中国科学院国家空间科学中心 复杂航天系统电子信息技术重点实验室，北京 100190）
3（中国科学院力学研究所，北京 100190）
4（中国科学院大学，北京 100049）
5（引力波宇宙太极实验室，浙江 杭州 310024）
6（浙江省引力波精密测量重点实验室，浙江 杭州 310024）
7（国科大杭州高等研究院 基础物理与数学科学学院，浙江 杭州 310024）
8（中国科学院工程热物理研究所，北京 100190）

摘 要：在基于外差干涉原理的空间引力波探测任务中，抖动光程耦合噪声是一个重要的光学噪声源，对测量系统的精度产生显著影响。本文提出了一种分析多种因素共同作用下抖动光程耦合噪声的方法。首先设计了一个等效的测试质量干涉仪仿真光学平台，并采用高斯光束追踪模拟光束传播。通过模拟干涉信号，可以分析各种因素对抖动光程耦合噪声的影响，包括位置因素、光束参数因素、探测器参数因素和信号定义因素。在此基础上，在满足分析要求的参数范围内,构建了由多个影响因素组成的随机参数空间，并通过基于方差的全局敏感性分析对随机采样得到的模拟结果进行评估。主要效应指数和总效应指数的计算结果表明，测试质量的旋转角度和活塞效应（径向）对测试质量干涉仪中的抖动光程耦合噪声有显著影响。这一结论为空间激光干涉测量系统的设计和优化提供了定性参考。

关键词：空间干涉测量；光学仿真；抖动光程耦合噪声

中图分类号：TP394.1；TH691.9　　**文献标识码：**A

1. Introduction

The detection of gravitational waves in space has gained significant international attention, driven by its ability to identify a wide range of detectable wave source frequencies and diverse types of wave sources. Several representative missions, such as Laser Interferometer Space Antenna (LISA) [1], Taiji [2], and Tianqin [3], are expected to launch in the next decade and achieve remarkable detection sensitivities. In those space-based gravitational wave detection missions, split heterodyne interferometry [4] is adopted, enabling the measurement of distance variations caused by gravitational waves between two test masses separated by millions of kilometers. The so-called science interferometers are utilized for measuring distance variations between satellites, while test mass interferometers are employed for measuring distance variations between the optical bench with respect to the test mass [4]. Notably, both types of interferometers are susceptible to a specific type of optical noise known as tilt-to-length (TTL) coupling noise, which arises due to beam tilt during measurement. The beam jitter received by the telescope in the science interferometer, and the rotation of the test mass the test mass interferometer, can lead to TTL coupling noise, for instance [5, 6]. Presently, it stands as the second most significant entry in the metrology error budget of LISA-like missions, following shot noise [7], hence, comprehending the characteristics of this noise fully is of paramount importance for effectively recognizing, suppressing, and subtracting the noise as needed.

Presently, researchers are directing their attention to two primary areas in investigating TTL coupling noise. The first aspect involves analyzing the factors that contribute to the noise, employing theoretical analysis or numerical simulation methods. Theoretical analysis of TTL coupling noise involves deriving analytical expressions of path length signals under various influential factors. Previous studies have provided qualitative and quantitative

explanations of both geometric [8, 9] and non-geometric mechanisms [10] of TTL coupling. Some research focused on specific conditions related to the cancellation of TTL and found that geometric optics alone is insufficient to describe the characteristics of TTL coupling noise accurately [8, 9]. Further studies explored the impacts of beam parameters [10, 11], signal definition [12] and wavefront aberrations [13-16] on TTL coupling noise. Requirements for telescope wavefront aberration [13-15] and the effect of low-order aberrations were also analyzed [16]. The second aspect entails exploring strategies to suppress the TTL coupling noise through optical design or data processing techniques for noise subtraction. Imaging systems have been effectively utilized for suppressing TTL coupling noise. Studies have demonstrated significant noise suppression using dual-lens or four-lens imaging systems can successfully suppress TTL coupling noise [6,7,17]. Additionally, simulations have provided insights into subtracting TTL coupling noise through linear regression methods and Bayesian inference [18-21].

The above research mainly focused on the derivation of analytical expressions for analyzing TTL coupling noise induced by individual factors, the development of imaging systems aimed at noise suppression, and the utilization of data processing techniques for noise extraction. The innovative contribution of this paper lies in its introduction of a methodology capable of analyzing multiple influential factors and discerning their individual impact by assigning a ranking. As a demonstration, we implement this methodology to the test mass interferometer of LISA-like mission.

Following this introduction, Section 2 introduces the definition of TTL coupling. In Section 3, the configuration for simulating TTL coupling is presented, and then the simulated results are compared with data obtained from an experiment. Subsequently, Section 4 presents the methodology for analyzing multiple influential factors. Based upon this, Section 5 delves into

the analysis that incorporates multiple factors using the simulation results. Finally, Section 6 summarizes the primary contributions of this paper and outlines future work.

2. The definition of TTL coupling

The fundamental nature of TTL coupling is the additional pathlength readout signal generated in the interferometer due to the jitter of the beam. Under the assumption of geometrical optics, where both interfering beams are considered as geometric rays, the noise can be defined by the optical path length difference (OPD) value. However, in actual interferometers, the interfering beams are not simple geometric rays. This implies that non-geometric effects cannot be disregarded. In such instances, any additional changes in path length will be detected by the detector of the interferometer using the longitudinal path length signal (LPS). In space-based gravitational wave detection missions, the quadrant photodiodes (QPD) are used as detectors, which have different combinations of signals from its four segments, resulting in various definitions for the LPS. Notably, the LPF (LISA pathfinder) and AP (averaged phase) definitions are widely employed [8]:

$$\mathrm{LPS}_{\mathrm{LPF}} = \frac{1}{k}\left(C_{\mathrm{A}} + C_{\mathrm{B}} + C_{\mathrm{C}} + C_{\mathrm{D}}\right) \tag{1}$$

$$\mathrm{LPS}_{\mathrm{AP}} = \frac{1}{4k}\left(\arg(C_{\mathrm{A}}) + \arg(C_{\mathrm{B}}) + \arg(C_{\mathrm{C}}) + \arg(C_{\mathrm{D}})\right) \tag{2}$$

where k represents the wavenumber ($2\pi/\lambda$), λ denotes the wavelength of the beam, meanwhile, the variables C_{A}, C_{B}, C_{C}, and C_{D} refer to the complex electric field on each quadrant of the QPD.

3. Simulation Method and Verification

To analyze TTL coupling noise, numerical simulations are implemented first and subsequently applied to the test mass interferometer. The results are

then validated through an experiment. This section primarily concentrates on the simulation of TTL coupling noise within the test mass interferometer. It is divided into two subsections. The first subsection outlines the simulation configuration utilized in this paper to simulate TTL coupling noise. The second subsection presents the comparison between the simulation results and experimental data, demonstrating the accuracy of the simulation.

3.1 Simulation Method

The software employed in this study for simulation purposes is one that we developed in [22], which addresses both geometric and non-geometric TTL coupling. For the simulation of the test mass interferometer, both the reference and measurement beams are treated as fundamental Gaussian beams. Their propagation can be easily described using the q-parameter and ray transfer matrix, which facilitates the computation of the complex electric field detected by the QPD, allowing for the determination of the LPS, i.e. Eq.(1) and Eq.(2).

Based on the concept of split heterodyne interferometry and the simulation software we developed, an equivalent simulated optical bench for the test mass interferometer has been designed, taking into account the motion of the freely suspended test mass, schematicly shown in Fig. 1. The beam from the laser is split into two beams by a beam splitter (BS). One beam serves as the reference beam, which is transmitted to the mirror (M) for reflection, while the other beam is directed towards the test mass and reflected off its surface. The reference beam and the measurement beam are then recombined at the beam splitter (BS) and interfere at the QPD.

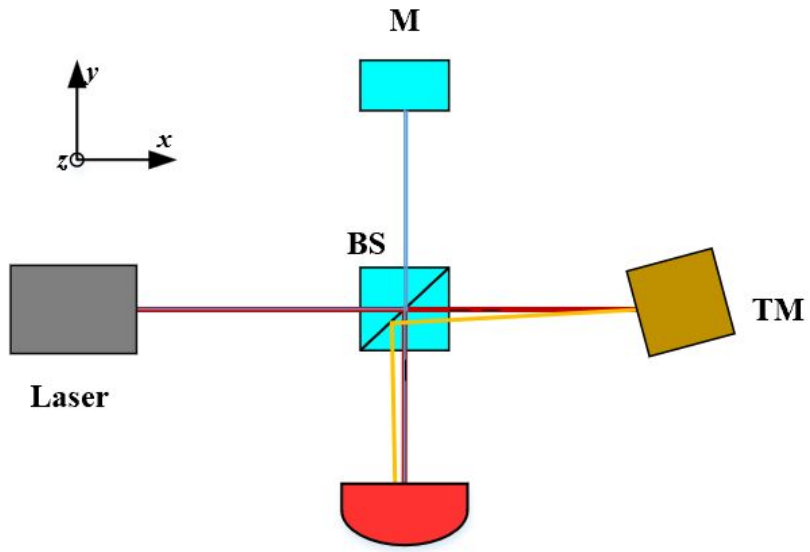

Fig. 1 Schematic diagram of the simulated optical bench for the test mass interferometer. The left upper corner shows the coordinate of the optical bench, with the detailed coordinates and normal vectors of every optical component are tabulated in the Table 1

Table 1 The type, position, and orientation of each component in the simulated optical bench used to analyze TTL coupling

Label	Component Name	Center coordinate *cm*	Normal Vector
Laser	Laser	(0,0,0)	(1,0,0)
BS	Beamsplitter	(25,0,0)	(-1,0,0)
M	Mirror	(25,50,0)	(0,-1,0)
TM	Test mass	(50,0,0)	(1,0,0)
QPD	Quadrant photodiode	(25,-25,0)	(0,1,0)

By employing this optical configuration, various factors affecting TTL coupling noise in the test mass interferometer can be simulated. The influential factors have been classified into four distinct categories: positional factors, beam parameters, detector parameters, and signal definition. Positional factors include beam offset, piston effect, test mass shift, and test mass rotation, as depicted in Fig. 2. The beam offset refers to the displacement between the measurement beam and the reference beam, caused by

misalignment. When the center of rotation of the test mass does not coincide with the reflection point of the beam on the test mass surface, the piston effect arises, which can be characterized by two parameters: the lateral parameter and the longitudinal parameter. In space-based gravitational wave detection, changes in the position and orientation of the test mass lead to TTL coupling. These changes are therefore considered as test mass shift and rotation angle. Beam parameters account for variations in beam waist and the distance from the waist of the measurement fundamental Gaussian beam. Regarding the detector parameter factor, TTL coupling noise arises because the signal cannot be fully detected due to the presence of slits in the QPD. This analysis focuses on the TTL coupling caused by QPD slits. The presence of QPD slits alters the definition of LPS. Unlike positional factors, beam parameters, and detector parameters, this type of factor affects TTL coupling not through input parameters but rather through how the detected signals are combined, as shown in Eq. (1) and Eq. (2).

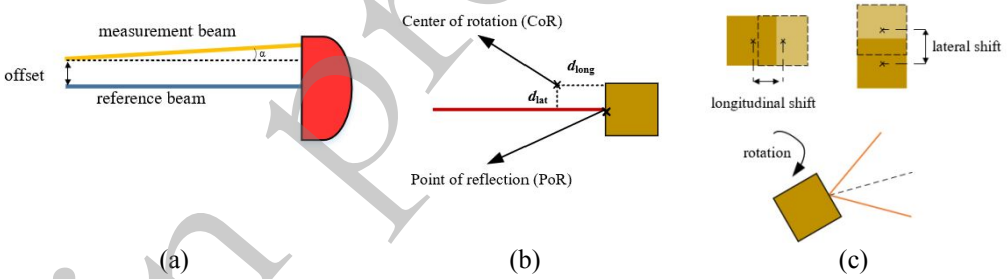

Fig. 2 Schematic illustration of positional factors: (a) the offset between the measurement and reference beam (b) the piston effect (c) the test mass shift and rotation

3.2 Simulation verification through an experiment

The simulation software developed and employed in this study has undergone verification with IfoCAD, a toolkit created by the Albert Einstein Institute, as discussed in [22]. To gain deeper insight into its accuracy, this subsection undertakes a comparative analysis between the simulation outcomes and experimental data.

The schematic illustration of the experimental setup is depicted in Figure 3. Both the measurement and reference beams, denoted by blue and red lines respectively, share identical beam parameters since they originate from the same laser. After passing through acousto-optical modulators (AOMs), their frequencies diverge. The reference beam is reflected by a stationary mirror labeled as "*Ref M*" in Figure 3, whereas the measurement beam is reflected by a fine steering mirror (FSM). The FSM is intentionally rotated to achieve the rotation of a test mass, where the center of rotation does not coincide with the beam's reflection point on the FSM surface. The detectors employed in this setup are four-channel phasemeters. Consequently, this experimental configuration results in a TTL signal arising from the piston effect when the FSM rotates.

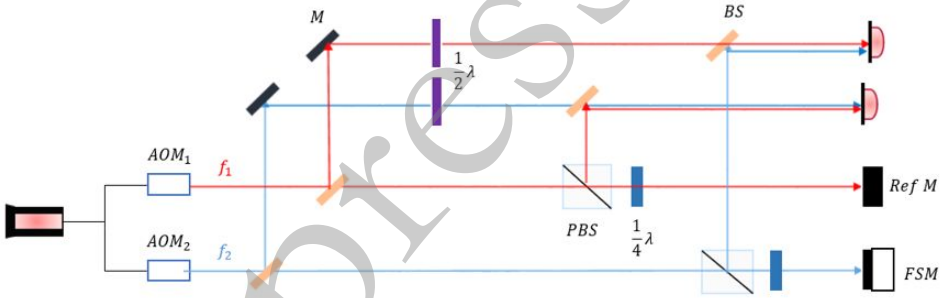

Fig.3 The schematic of the experimental setup, components included: acousto-optical modulator (AOM), polarizing beam splitter (PBS), half wave plate (λ/2), quarter wave plate (λ/4), beam splitter (BS), stationary mirror (Ref M), fine steering mirror (FSM)

The simulation utilizes the experimental parameters to compute the LPS signal, adopting the same rotation angles as those used in the experiment. Table 2 outlines the physical parameters involved. Subsequently, the experimental and simulation data are graphically represented in Figure 4, and Table 3 provides the relative error of the LPS for various rotation angles.

Table 2 Physical parameters list

Parameter description	Value
reference beam waist	0.5 mm

distance from waist of reference beam	0
reference beam frequency	2.8195×10^8 MHz +120 MHz
measurement beam waist	0.5 mm
distance from waist of measurement beam	0 mm
measurement beam frequency	2.8195×10^8 MHz +120 MHz+1.6 MHz
QPD radius	1 cm
QPD slit size	50 μm

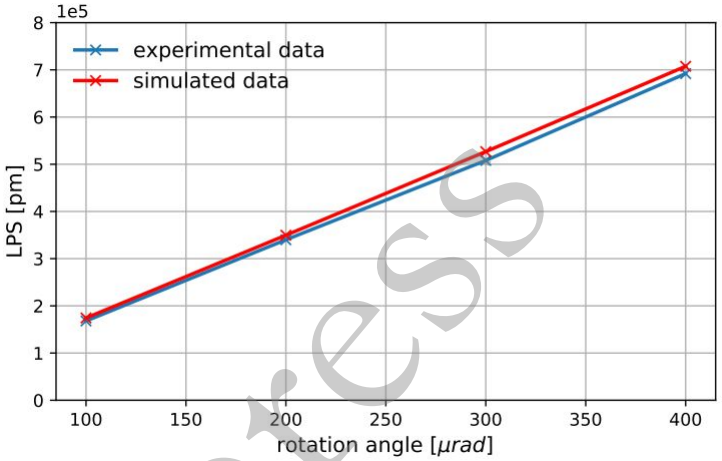

Fig.4 Comparison of experimental data and simulation data

Table 3 Comparison of rotation angle (μrad) and relative error (%)

Rotation Angle (μrad)	Relative Error (%)
100	3.78
200	2.84
300	3.69
400	2.24

The average relative error between the simulation results and experimental data has been calculated to be 3.14%. The discrepancies observed in TTL coupling noise between the simulated and experimental data can be attributed to several factors. Firstly, the simulation model may incorporate assumptions and simplifications that fail to fully encapsulate the

intricacies and non-ideal aspects of the actual system. Secondly, experimental conditions, such as environmental disturbances, which were not accounted for, may introduce measurement errors. Additionally, the precision of the system parameters and the accuracy of the simulation model itself can further affect the consistency between the two datasets.

4. Analysis method for multiple factors

In practical applications, TTL coupling noise typically arises due to the combined influence of multiple factors. When these factors act simultaneously, analyzing the LPS becomes a complex and challenging task. In such cases, numerical simulation offers a viable alternative approach. Through employing numerical simulation introduced in Section 3, it is possible to comprehensively analyze the effects of various factors on TTL coupling noise and obtain accurate estimations of the LPS. This simulation-based approach provides valuable insights into the behavior and characteristics of TTL coupling noise in real-world scenarios, enabling researchers to develop effective strategies for its recognition, suppression, and subtraction in practical applications.

The analysis method for multiple factors is built on the fundamental concept of employing random parameters within a defined and reasonable range which affect the TTL coupling. By generating a diverse set of random parameter combinations, the simulation captures the variability of real-world scenarios. Based on the simulation, the variance-based global sensitivity analysis method is utilized to assess the sensitivity of the TTL coupling noise to each parameter. The analysis calculates the main effect index S_1 and the total effect index S_T for each parameter, providing quantitative measurements of their influences on the TTL coupling noise. Therefore, this method enables the identification of the key factors that significantly impact TTL coupling noise when multiple factors operate simultaneously. By systematically

examining the main and total effect indices, researchers can prioritize the factors that contribute the most to TTL coupling noise and focus their efforts on mitigating their impact.

The main effect index S_1 quantifies the extent to which an individual influential factor, x_i contributes to the variation in the output variance of the system. A higher S_1 value indicates a stronger influence of that particular factor on the TTL coupling noise. On the other hand, the total effect index S_T assesses the collective contribution of each influential factor to the overall variation in the output variance. This index takes into account both the direct effect of the factor and its interactions with other factors. A larger S_T value indicates a more significant combined influence of all the factors on the TTL coupling noise. By evaluating both S_1 and S_T, researchers can gain a comprehensive understanding of the relative importance and impact of each influential factor, enabling them to prioritize and address the critical factors in their efforts to suppress TTL coupling noise. It should be noted that S_1 and S_T serve as indicators of the relative importance of various factors affecting TTL coupling noise, rather than direct measures of the impact on the final design accuracy of the interferometer.

The calculations of S_1 and S_T are calculated as follows [23-24]:

$$S_1 = \frac{V_{x_i}\left(E_{x_i}(y \mid x_i)\right)}{V(y)} \tag{3}$$

$$S_T = \frac{E_{x_{\sim i}}\left(V_{x_i}(y \mid x_{\sim i})\right)}{V(y)} \tag{4}$$

where V represents variance, E represents mathematical expectation, and x_i represent the i-th influential factor , with ~ indicating all influential factors except the i-th. y represent the corresponding LPS.

To address the challenges in directly calculating equations Eq. (3) and Eq. (4), commonly employed approximation methods are utilized [25-26]:

$$V_{x_i}\left(E_{x_i}(y \mid x_i)\right)=\frac{1}{N}\sum_{j=1}^{N} f(B)_j\left(f(AB_i)_j-f(A)_j\right) \tag{5}$$

$$E_{x_{\sim i}}\left(V_{x_i}(y \mid x_{\sim i})\right)=\frac{1}{2N}\sum_{j=1}^{N}\left(f(A)_j-f(AB_i)_j\right)^2 \tag{6}$$

The step-by-step algorithm for analyzing multiple factors is as follows:

Step 1: Randomly generating a sampling matrix of size $N\times 2n$ in the parameter space, where N is the number of sampling points and n is the number of parameters which influence the TTL coupling noise.

Step 2: Using the first n columns of the $N\times 2n$ matrix as matrix A and the last n columns as matrix B. The parameter order of matrix B must be consistent with that of matrix A.

Step 3: Constructing a matrix AB_i of size $N\times n$, where i = 1, 2,..., n. The i-th column of AB_i is the i-th column of matrix B, and the other columns are the columns of matrix A except for the i-th column.

Step 4: Calculating the corresponding LPS for random parameter matrices A, B, and AB_i.

Step 5: Calculating the main effect index and total effect index based on Eq. (5) and Eq. (6).

5. Results and analysis

In this section, the method introduced in Section 4, is employed to analyze the characteristics of TTL coupling noise when multiple factors act simultaneously. The simulated optical setup presented in this section is illustrated in Fig. 1.

The first step is to generate a sampling matrix containing parameters influencing TTL coupling. For convenience, Table 4 presents the parameter space, detailing the range of each parameter, which satisfies the requirements of Taiji.

Table 4 Parameter space for multiple factor analysis

Factors	Parameter	Range
Positional	beam offset	(0 μm, 100 μm)
	piston effect -lateral	(0 mm, 1 mm)
	piston effect -longitudinal	(0 mm, 1 mm)
	test mass lateral shift	(0 μm, 100 μm)
	test mass longitudinal shift	(0 μm, 100 μm)
	rotation angle	(0 μrad, 100 μrad)
Beam parameter	Measurement beam waist	(0.5mm, 1 mm)
	the distance from the waist of the measurement beam	(0 mm, 50 mm)
Detector parameter	QPD slit	(0 μm, 100 μm)

For 10,000 simulations, parameters were randomly chosen from the parameter space with a uniform distribution, the corresponding LPS are computed using both LPF and AP definitions, and their respective histograms are illustrated in Fig. 5.

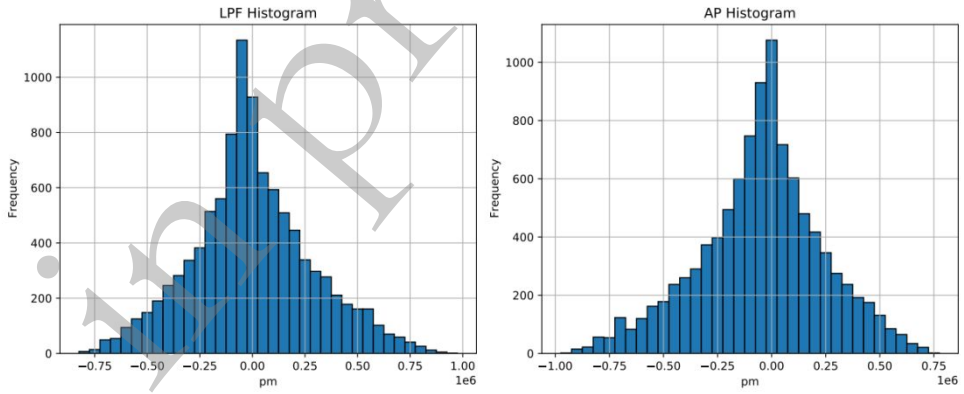

Fig. 5 Histograms of LPS with LPF and AP definition in 10000 simulations

Based on the simulation results, the LPS using the AP definition spans a range from -9.1285×10^5 pm to 7.6925×10^5 pm, while the range is -7.9348×10^5 pm to 9.6939×10^{5}pm with the LPF definition. Fig. 3. also indicates that the highest range of LPS signal with the LPF definition is from -1×10^5 pm to 0 pm

(1033 occurrences), whereas for the AP definition, this range is from 0 to 1×10^5 pm (1088 occurrences). Within the 10000 simulations, the maximum absolute value and minimum absolute value for both signal definitions are detailed in Table 5.

Table 5 Maximum (absolute value) and minimum (absolute value) of the LPS with both LPF and AP in 10000 simulations.

Signal definition	Maximum	Minimum
LPF	9.6939×10^5 pm	6.4400 pm
AP	9.1285×10^5 pm	14.7801 pm

From Table 4, it is evident that the minimum absolute value of LPS is approximately 10 pm under both signal definitions. However, it should be noted that while setting parameter values may theoretically result in minimal noise, the practical feasibility of achieving such conditions remains uncertain.

Subsequently, the simulation data can be utilized to compute the main effect index S_1 and the total effect index S_T for both signal definitions. The results are presented in Table 5 and Table 6, respectively, and are also depicted visually in Figure 6 and Figure 7 to provide a clear and intuitive representation.

Table 6 Main effect index S_1 and total effect index S_T for different parameters (LPF definition)

Factors	Parameter	S_1	S_T
Positional	beam offset	0.00037	0.00023
	piston effect -lateral	0.01516	0.21815
	piston effect -longitudinal	8.8911×10^{-7}	5.3478×10^{-9}
	test mass lateral shift	-0.00096	0.00217
	test mass longitudinal shift	-1.0968×10^{-7}	5.9016×10^{-11}
	rotation angle	0.75350	0.99122
Beam parameter	Measurement beam waist	0.00081	0.00240
	the distance from the waist of the measurement beam	5.8822×10^{-6}	3.1740×10^{-7}
Detector parameter	QPD slit	0.00017	0.00028

Table 7 Main effect index S_1 and total effect index S_T for different parameters (AP definition)

Factors	Parameter	S_1	S_T
Positional	beam offset	0.00093	0.00047
	piston effect -lateral	0.01409	0.21586
	piston effect -longitudinal	1.6607×10^{-6}	5.29173×10^{-9}
	test mass lateral shift	-0.00117	0.00214
	test mass longitudinal shift	-1.6703×10^{-7}	7.6198×10^{-11}
	rotation angle	0.75988	0.99156
Beam parameter	Measurement beam waist	0.00085	0.00039
	the distance from the waist of the measurement beam	2.1826×10^{-6}	5.2593×10^{-8}
Detector parameter	QPD slit	0.00073	0.00035

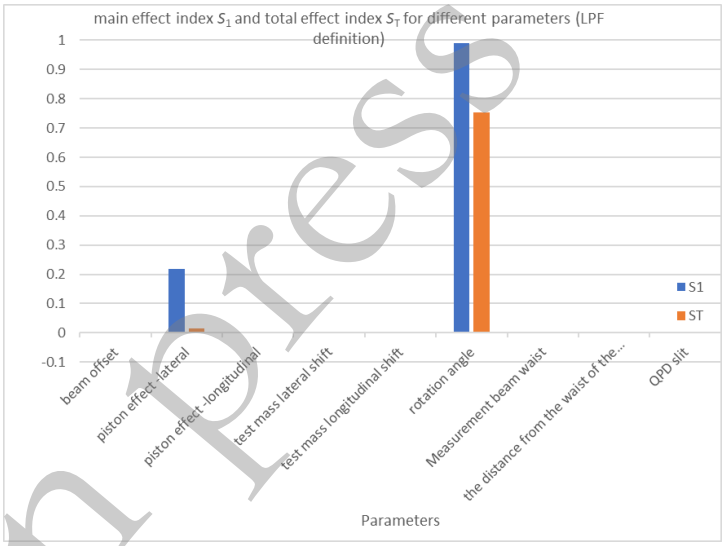

Fig. 6 Visualization of the main effect index (S_1) for LPF definition

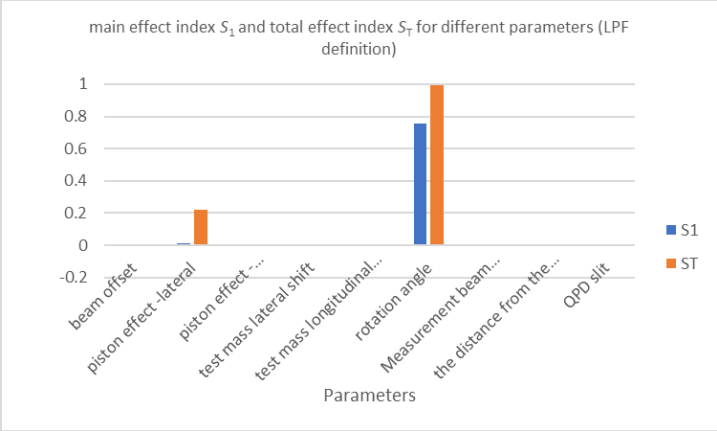

Fig. 7 Visualization of the total effect index (S_T) for AP definition

As is mentioned before, the role of S_1 is to rank the importance of input variables. When the LPF definition is used, the rank of S_1 in descending order is: rotation angle, piston effect -lateral, test mass lateral shift, measurement beam waist radius, measurement beam offset, QPD slit, measurement beam waist position, piston effect -longitudinal, and test mass longitudinal shift. As for the AP definition, the rank of S_1 in descending order is: rotation angle, piston effect -lateral, test mass lateral shift, measurement beam offset, measurement beam waist radius, QPD slit, measurement beam waist position, piston effect -longitudinal, and test mass longitudinal shift. It can be seen that there is no significant difference in the order of S_1 between the two definitions.

On the other hand, S_T serves to simplify the model parameters. When the LPF definition is applied, the value of S_T in descending order is: rotation angle, piston effect -lateral, measurement beam waist radius, test mass lateral shift, QPD slit, measurement beam offset, measurement beam waist position, piston effect -longitudinal, and test mass longitudinal shift. For the AP definition, the rank of S_T in descending order is: rotation angle, piston effect -lateral, test mass lateral shift, measurement beam waist radius, measurement beam offset, QPD slit, measurement beam waist position, piston effect -longitudinal, and test mass longitudinal shift. It can be seen that S_1 and S_T of LPF definition have slightly different rankings, but the overall trend is roughly the same,

while for the AP definition, the S_1 and S_T rankings defined by AP are exactly the same.

According to the analysis of S_1 and S_T, it can be concluded that regardless of which signal definition is used, the S_1 and S_T values of rotation angle and piston effect -lateral are much larger than those of other factors. Therefore, these two factors have the greatest impact on LPS. Additionally, the effects of measurement beam waist position, piston effect -longitudinal, and testing mass longitudinal shift on LPS are small. For further analysis, the parameter space was expanded by 50% and reduced by 50%, and the main effect index S_1 and the total effect index S_T were calculated again. The conclusion remained the same. This means that in practice, efforts should be made to control the rotation of the test mass and keep its center of the test mass as close as possible to its geometric center to reduce piston effect.

6. Conclusion

This paper proposes a method to analyze the impacts of multiple factors on TTL coupling noise using random parameters. A simulated optical bench is constructed based on the principle of test mass interferometer, supporting the simulation of various noise-affecting factors, and validated with experimental data. The simulation and analysis cover positional factors, beam parameters, detector parameters, and signal definition. With parameters randomly drawn from reasonable ranges, 10000 simulations are carried out. Then the simulation data are used for the variance-based global sensitivity analysis, where sensitivity indices are calculated to identify the key factors impacting TTL coupling noise, namely, test mass rotation angle and piston effect -lateral. This conclusion offers key knowledge for system design and optimization. The forthcoming research will primarily concentrate on the practical application of the proposed method to study TTL coupling noise in science

interferometers. Additionally, experiments will be conducted to verify the accuracy of the analysis results obtained through this method.

References:

[1] P. Amaro-Seoane, H. Audley, S. Babak, et al., "Laser interferometer space antenna," *arXiv preprint arXiv:1702.00786* (2017).

[2] Z. LUO, M. ZHANG, G. JIN, et al., "Introduction of Chinese space-borne gravitational wave detection program "Taiji" and "Taiji-1" satellite mission," J*ournal of Deep Space Exploration* 7(1), 3 – 10 (2020).

[3] J. Luo, L. S. Chen, H. Z. Duan, et al., "Tianqin: a space-borne gravitational wave detector," *Classical and Quantum Gravity* 33(3), 035010 (2016).

[4] M. Otto, Time-delay interferometry simulations for the laser interferometer space antenna. PhD thesis, Gottfried Wilhelm Leibniz Universität Hannover (2015).

[5] S. Schuster, G. Wanner, M. Tröbs, et al., "Vanishing tilt-to-length coupling for a singular case in two-beam laser interferometers with gaussian beams," *Applied Optics* 54(5), 1010 – 1014 (2015).

[6] L. Y. Wang, Y. Q. Li, and R. Cai, "Noise suppression of tilt-to-length coupling in space laser interferometer," *Optics and Precision Engineering* 29(7), 1491 (2021).

[7] M. Chwalla, K. Danzmann, G. F. Barranco, et al., "Design and construction of an optical test bed for lisa imaging systems and tilt-to-length coupling," *Classical and Quantum Gravity* 33(24), 245015 (2016).

[8] S. Schuster, Tilt-to-length Coupling and Diffraction Aspects in Satellite Interferometry. PhD thesis, Gottfried Wilhelm Leibniz Universität Hannover (2017).

[9] M. S. Hartig, S. Schuster, and G. Wanner, "Geometric tilt-to-length coupling in precision interferometry: mechanisms and analytical descriptions," *Journal of Optics* 24(6), 065601(2022).

[10] M. S. Hartig, S. Schuster, G. Heinzel, et al., "Non-geometric tilt-to-length coupling in precision interferometry: mechanisms and analytical descriptions," *Journal of Optics* 25(5), 055601 (2023).

[11] Y. Zhao, Z. Wang, Y. Li, et al., "Method to remove tilt-to-length coupling caused by interference of flat-top beam and gaussian beam," *Applied Sciences* 9(19), 4112 (2019).

[12] G. Wanner, S. Schuster, M. Tröbs, et al., “A brief comparison of optical pathlength difference and various definitions for the interferometric phase,” *Journal of Physics: Conference Series* 610(1), 12043 (2015).

[13] C. P. Sasso, G. Mana, and S. Mottini, “Coupling of wavefront errors and pointing jitter in the lisa interferometer: Misalignment of the interfering wavefronts,” *Classical and Quantum Gravity* 35(24) (2018).

[14] Y. Zhao, J. Shen, C. Fang, et al., “Tilt-to-length noise coupled by wavefront errors in the interfering beams for the space measurement of gravitational waves,” *Optics Express* 28(17), 25545-25561 (2020).

[15] Y. Zhao, J. Shen, C. Fang, et al., “The far-field optical path noise coupled with the pointing jitter in the space measurement of gravitational waves,” *Applied Optics* 60(2) (2020).

[16] J.-c. LI, H.-a. LIN, J.-x. LUO, et al., “Optical design of space gravitational wave detection telescope,” *Chinese Optics* 15(4), 761 (2022).

[17] S. Schuster, M. Tröbs, G. Wanner, et al., “Experimental demonstration of reduced tilt-to-length coupling by a two-lens imaging system,” *Optics Express* 24(10), 10466 (2016).

[18] A. J. Weaver, “Investigating limits on gravitational wave detection by laser interferometry using hermite-gauss mode representations of paraxial light propagation,” Ph.D. Thesis, University of Florida (2021).

[19] Paczkowski, S., et al. “Postprocessing subtraction of tilt-to-length noise in LISA.” *Physical Review D* 106.4 (2022): 042005.

[20] Houba, Niklas, et al. “Optimal estimation of tilt-to-length noise for spaceborne gravitational-wave observatories.” *Journal of Guidance, Control, and Dynamics* 45.6 (2022): 1078-1092.

[21] George, Daniel, et al. “Calculating the precision of tilt-to-length coupling estimation and noise subtraction in LISA using Fisher information.” *Physical Review D* 107.2 (2023): 022005.

[22] Mengyuan Zhao, Xiaodong Peng, Zhen Yang, Xin Meng, Xiaoshan Ma, Jiafeng Zhang, “Preliminary simulation of intersatellite laser interference link for the Taiji program,” *J. Astron. Telesc. Instrum. Syst.* 8(3) 038002 (2022).

[23] I. M. Sobol’, “On sensitivity estimation for nonlinear mathematical models,” *Matematicheskoe modelirovanie* 2(1), 112–118 (1990).

[24] T. Homma and A. Saltelli, “Importance measures in global sensitivity analysis of nonlinear models,” *Reliability Engineering & System Safety* 52(1), 1-17 (1996).

[25] I. M. Sobol, “Global sensitivity indices for nonlinear mathematical models and their monte carlo estimates,” *Mathematics and computers in simulation* 55(1-3), 271–280 (2001).

[26] A. Saltelli, P. Annoni, I. Azzini, et al., “Variance based sensitivity analysis of model output. design and estimator for the total sensitivity index,” *Computer physics communications* 181(2), 259–270 (2010).

Author biographies:

Zhao Mengyuan(1996-), a PhD graduate from Key Laboratory of Electronics and Information Technology for Space System in the National Space Science Center, Chinese Academy of Sciences, and is currently employed at the School of Information, Xi’an University of Finance and Economics. Her research interest is the high-precision simulation, analysis, and evaluation of space missions. E-mail: 2023010027@xaufe.edu.cn

Ma Xiaoshan, a professor at Institute of Engineering Thermophysics, Chinese Academy of Sciences. Her research interest is combustion diagnostic technology. E-mail: maxiaoshan@iet.cn